

SRI Report No. 951581-7

POST-TEST ANALYSIS OF GENERANT TANK, PART NO. 9116270-H

Prepared for:

JET PROPULSION LABORATORY
CALIFORNIA INSTITUTE OF TECHNOLOGY
PASADENA, CALIFORNIA 91103

JPL CONTRACT 951581
UNDER NAS7-100

STANFORD RESEARCH INSTITUTE

MENLO PARK, CALIFORNIA



FACILITY FORM 602

N 68-25107
(ACCESSION NUMBER) (THRU)

38
(PAGES) (CODE)

CI-94765
(NASA CR OR TMX OR AD NUMBER) (CATEGORY)

15

GPO PRICE \$ _____

CFSTI PRICE(S) \$ _____

Hard copy (HC) 3.00

Microfiche (MF) 65

ff 653 July 65

STANFORD RESEARCH INSTITUTE

MENLO PARK, CALIFORNIA



April 15, 1968

SRI Report No. 951581-7

POST-TEST ANALYSIS OF GENERANT TANK, PART NO. 9116270-H

Prepared for:

JET PROPULSION LABORATORY
CALIFORNIA INSTITUTE OF TECHNOLOGY
PASADENA, CALIFORNIA 91103

JPL CONTRACT 951581
UNDER NAS7-100

JPL Technical Representative: H. B. STANFORD
JPL Technical Cognizance: L. R. TOTH

By: R. F. MURACA A. E. BAYCE C. H. MARTIN J. S. WHITTICK

SRI Project: ASD-6063

Approved: R. F. MURACA, DIRECTOR
ANALYSES AND INSTRUMENTATION

**This work was performed for the Jet Propulsion Laboratory,
California Institute of Technology, sponsored by the
National Aeronautics and Space Administration under
Contract NAS7-100.**

Copy No. 15

ABSTRACT

A post-test analysis has been made of the prototype spacecraft generant tank, Part No. 9116270-H, which had been subjected to intermittent testing with hydrazine and gaseous nitrogen at internal pressures up to 1500 psi and temperatures of less than 150⁰F.

The analysis of the titanium hemisphere, including mechanical property determinations and metallographic examination revealed that no deterioration of properties had occurred during test and that the fabrication was sound.

The analysis of the ethylene-propylene expulsion diaphragm indicated that some embrittlement of the elastomer had occurred, accompanied by an apparent loss in tensile strength. The rate of permeation to hydrazine, however, was not significantly different from an equivalent manufacturer's sample.

CONTENTS

ABSTRACT ii
TABLES iv
ILLUSTRATIONS v

I INTRODUCTION 1

II EPR DIAPHRAGM ANALYSIS 5
 Chemical and Physico-Chemical Determinations 5
 Mechanical Property Tests 7

III TITANIUM TANK ANALYSIS 13
 Metallography 13
 Mechanical Property Determinations 16

IV SUMMARY AND CONCLUSIONS 29

REFERENCES 31

TABLES

Table 1	Results of Qualitative Analyses for Cations in EPR SR722-70 After Test	9
Table 2	Effect of Substances Extracted from Test EPR SR722-70 on the Decomposition of Hydrazine at 125°F	9
Table 3	Permeability of EPR SR722-70 at 72°F to Hydrazine at One Atmosphere	9
Table 4	Density Determinations of EPR SR722-70 after Test	10
Table 5	Shore A Hardness Determinations for EPR SR722-70	10
Table 6	Tensile and Elongation Values for EPR SR722-70	10
Table 7	Mechanical Properties of Selected Areas of Ti-6Al-4V Generant Tank	18
Table 8	Microhardness Measurements of Parent Metal and Welded Metal in 6Al-4V Titanium Hemisphere	18

ILLUSTRATIONS

Fig. 1	External Appearance of Generant Tank Assembly, Part No. 9116270-H as Received at SRI	3
Fig. 2	Internal Appearance of Generant Tank Assembly as Received at SRI; the View Shows the Side of the Diaphragm-Type Bladder Which was Exposed to Nitrogen . . .	3
Fig. 3	View of Tank Assembly at Girth Weld	4
Fig. 4	Photograph of the EPR diaphragm (Hydrazine-Side) Cut Away from the Titanium Hemisphere	11
Fig. 5	Photograph of the Internal Area of Generant Tank; Note Discoloration Related to Diaphragm-Rib Marks and Other Spotty Deposits	11
Fig. 6	Location of Sampling Areas for EPR Diaphragm Analyses . . .	12
Fig. 7	Permeability Apparatus	12
Fig. 8	Location of Metallography Specimens	19
Fig. 9	Location of Titanium Tensile Specimens	19
Fig. 10	Cross-Section of Generant Tank Outlet Port and Barrier Plate; Magnification, 5X. (Macroetch, 1 HF, 1.5 HCl, 2.5 HNO ₃ , 95 H ₂ O)	20
Fig. 11	Bottom View of Sieve-Like Barrier Leading to Generant Tank Outlet Port; Magnification, 2X. (Macroetch, 1 HF, 1.5 HCl, 2.5 HNO ₃ , 95 H ₂ O)	21
Fig. 12	Cross-Section through Girth Weld Area; Magnification, 2.5X. (Macroetch, 1 HF, 1.5 HCl, 2.5 HNO ₃ , 95 H ₂ O)	21
Fig. 13	Photomicrograph of Transverse Cross-Section of Hemisphere away from the Weld Area; Magnification, 250X. (Etchant, 1 HF, 4 HNO ₃ , 95 H ₂ O, swab 10 seconds)	22

Fig. 14	Photomicrograph of Transverse Cross-Section of Hemisphere away from the Weld Area; Magnification, 1000X	22
Fig. 15	Photomicrograph of Longitudinal Cross-Section away from the Weld Area; Magnification, 250X. (Etchant: 1 HF, 4 HNO ₃ , 95 H ₂ O, swab 10 seconds)	23
Fig. 16	Photomicrograph of Longitudinal Cross-Section away from the Weld Area; Magnification, 1000X	23
Fig. 17	Macrophoto of Longitudinal Section through Girth Weld; Magnification, 8X. (Etchant: 1 HF, 4 HNO ₃ , 95 H ₂ O, swab 10 seconds)	24
Fig. 18	Photomicrograph at Center Line of Longitudinal Section through Girth Weld; Magnification, 20X. (Etchant: 1 HF, 4 HNO ₃ , 95 H ₂ O, swab 10 seconds)	24
Fig. 19	Photomicrograph of Longitudinal Section through Girth Weld; Magnification, 200X	25
Fig. 20	Photomicrograph of Longitudinal Section through Girth Weld; Magnification, 1000X	25
Fig. 21	Macrophoto of Transverse Cross-Section of Girth Weld; Wall of Hemisphere to the Left and Back-Up Ring on the Right; Magnification, 8X. (Etchant: 1 HF, 4 HNO ₃ , 95 H ₂ O, swab 10 seconds)	26
Fig. 22	Photomicrograph of Girth Weld at Joint Area between Wall of Hemisphere and Back-Up Ring; Magnification, 20X. (Etchant: 1 HF, 4 HNO ₃ , 95 H ₂ O)	26
Fig. 23	Photomicrograph of Edge of Heat-Affected Zone of Weld Shown in Figure 22; Magnification, 200X. (Etchant 1 HF, 4 HNO ₃ , 95 H ₂ O)	27
Fig. 24	Photomicrograph of Girth Weld; Magnification, 200X. (Etchant: 1 HF, 4 HNO ₃ , 95 H ₂ O, swab 10 seconds)	27
Fig. 25	Photomicrograph of Girth Weld; Magnification, 1000X.	28
Fig. 26	Dimensions of Titanium Tensile Test Specimens	28

I. INTRODUCTION

The post-test analysis of a section of an experimental spacecraft generant tank assembly (Part No. 9116270-H) was undertaken by Stanford Research Institute in response to a request by the Jet Propulsion Laboratory for an examination to determine whether the metal portion of the tank and its diaphragm assembly were deteriorated in any way during storage with hydrazine and gaseous nitrogen at internal pressures up to 1500 psi and temperatures of less than 150°F. The ultimate objective of the analysis was to provide significant information for material compatibility and design evaluation.

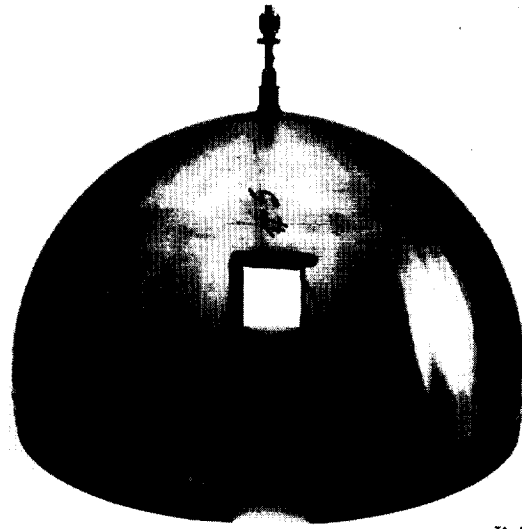
The sub-assembly submitted to SRI was a 6Al-4V titanium hemisphere (17-inch diameter) in annealed condition containing a bonded diaphragm-type expulsion bladder made of ethylene-propylene co-polymer (Stillman Rubber Company, No. SR722-70). Figures 1 and 2 are photographs of the sub-assembly as received at SRI; the areas cut away were removed by JPL. The internal view (Figure 2) shows the side of the diaphragm which was exposed to nitrogen. The series of spots seen about the rim of the hemisphere in Figure 2 are the remains of temperature-sensitive tapes used to indicate welding temperatures during fabrication. A detail of the girth-weld and bonding of the diaphragm to the titanium hemisphere is shown in Figure 3.

The generant tank was designed to meet the specifications quoted in JPL Spec. No. 30209 [1], and the complete assembly with the expulsion diaphragm was fabricated according to JPL Reference Drawing No. 9116270, Revision H; the diaphragm was secured to the girth of the tank by special welding techniques developed for JPL [2]. The generant tank was subjected to storage and expulsion tests at intervals during the period April 1965 to November 1966. After each test, the hydrazine and nitrogen were expelled completely. The surfaces of metal and elastomer exposed to hydrazine were flushed with distilled water and dried under vacuum.

Prior to fabrication of this test generant tank, detailed investigations of the compatibility of polymers and metals with hydrazine [3] were made by JPL.

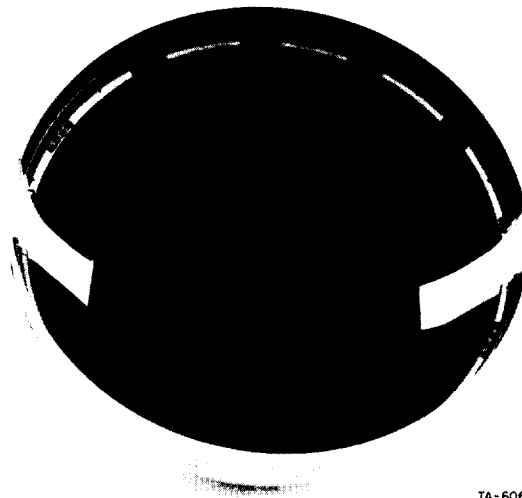
At the outset of the post-test analysis by SRI, a preliminary examination was made of the tank assembly by analytical chemists, metallurgists, and machinists. The examination revealed no obvious corrosion or defects of metal at the girth weld line or at the cross-sections exposed by the sampling cuts made at JPL; the diaphragm material was intact and well-bonded, with a uniform surface area apparently free of defects. The weld seam appeared intact with no immediately discernible pin-holes. Subsequent to the preliminary examination and a review of JPL reports, specifications, and drawings, it was determined that the most useful information would be derived from comparative testing of specimens of the metallic and polymeric materials taken from areas near the girth weld and well away from the girth weld, since no original samples of the SR722-70 EPR polymer or the 6Al-4V titanium alloy were provided for comparison.

The diaphragm analyses (Section II) included mechanical property determinations and physico-chemical determinations. The metallurgical analyses (Section III) included metallography and mechanical property determinations. Conclusions and recommendations based on the analyses are given in Section IV.



TA-6063-115

FIG. 1 EXTERNAL APPEARANCE OF GENERANT TANK ASSEMBLY,
PART NO. 9116270-H, AS RECEIVED AT SRI



TA-6063-116

FIG. 2 INTERNAL APPEARANCE OF GENERANT TANK ASSEMBLY AS RECEIVED
AT SRI; THE VIEW SHOWS THE SIDE OF THE DIAPHRAGM-TYPE
BLADDER WHICH WAS EXPOSED TO NITROGEN

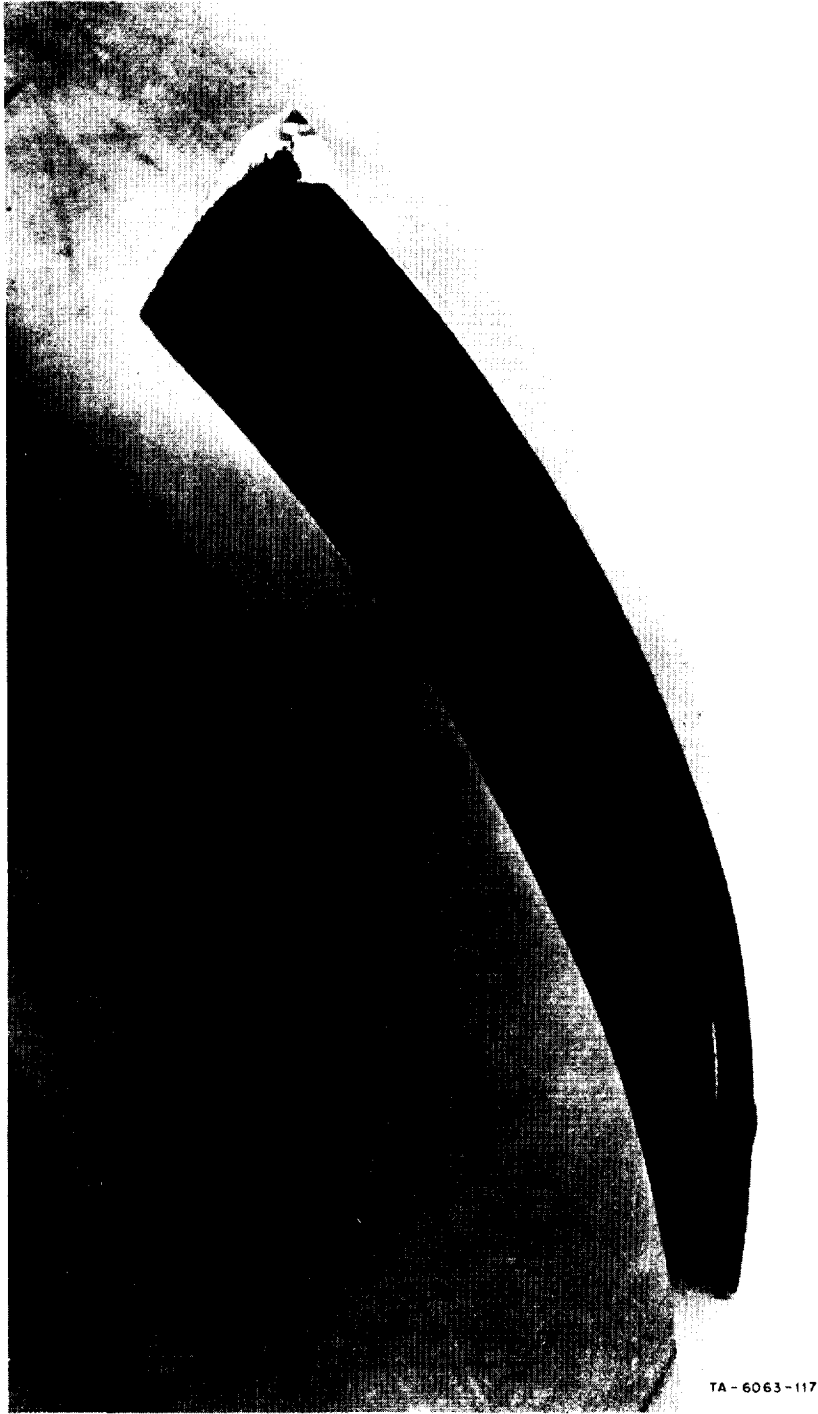


FIG. 3 VIEW OF TANK ASSEMBLY AT GIRTH WELD

II. EPR DIAPHRAGM ANALYSIS

The EPR diaphragm-type bladder was cut away from the titanium hemisphere along the girth weld line with a razor edge; care was taken to cut the elastomer close to the seam without scarring the titanium surface. A photograph of the side of the diaphragm which had been exposed to hydrazine is shown in Figure 4. Deposits of dark-colored material were found on the inner walls of the titanium hemisphere (shown in Figure 5) as distinct lines related to the rest-positions of the ribbed portions of the diaphragm and as occasional spots in-between the rib marks. This suggests that the hydrazine had leached colored substances out of the ethylene-propylene diaphragm.

The thickness of the diaphragm varied from 0.039" at the girth weld to 0.093" at the dome, furthest away from the weld line, in accordance with the JPL studies [2] which indicated that the area in the vicinity of the outlet barrier plate should be thicker by a factor of 2.

As indicated in Figure 6, test samples of the diaphragm were taken from the areas near the girth weld and away from the girth weld; samples for density were taken from the side exposed to nitrogen and from the side exposed to hydrazine. A composite sample of material taken from numerous sections of the diaphragm was used to determine whether there are residual extractable substances which enhance the rate of decomposition of hydrazine.

CHEMICAL AND PHYSICO-CHEMICAL DETERMINATIONS

Metallic Impurities or Additives

Qualitative analyses for several cations were performed on samples of the diaphragm material taken from the areas shown in Figure 6; the selection of cations to be detected was based on prior experience with similar EPR polymers. The samples were digested in concentrated sulfuric acid, neutralized with ammonium hydroxide, filtered to remove carbonaceous

material, and then heated at 400°C overnight to remove ammonium sulfate. The cations listed in Table 1 were detected in the residues by spot tests. The tests were qualitative, but it was readily apparent that the calcium and zinc concentrations were high. The fact that titanium was present in the sample near the girth weld and not in the area away from the girth weld might indicate that titanium had been transferred to the EPR during welding (probably as the condensed metallic vapor or a compound such as the oxide^{*}).

Extractable Substances

Extractable substances must be considered as possible contributors to hydrazine decomposition under long-term storage. About 3 grams of finely-cut diaphragm material were stored in a glass-stoppered bottle with 15 cc of hydrazine for a two-week period at room temperature. Then, the hydrazine, now brownish-yellow in color but free of any precipitate, was decanted, and then sealed in an acid-cleaned glass capsule fitted with a break-off seal. This test capsule was stored for 48 hours at 125°F; a capsule containing fresh hydrazine was stored concurrently as a control sample.

After storage, pressure in the test capsules was measured and the noncondensable gases at -196°C were analyzed mass spectrometrically. The analysis showed that noncondensable gases consisted primarily of nitrogen, with some hydrogen; ullage pressures at -196°C were essentially the same for both the control sample and the sample containing the EPR extract (see Table 2). The presence of nitrogen at -196°C (and ammonia at -78°C) indicated that some decomposition had taken place in both samples and that no acceleration of decomposition could be attributed to the presence of substances extracted from the EPR diaphragm.

* Inert gas atmospheres used for welding contain small amounts of oxygen; even the residual gas in the high vacuum required for electron-beam welding contains sufficient oxygen for reaction with titanium.

Permeability

The permeabilities to hydrazine of selected sections of the bladder material were determined essentially according to the "Vango" method: The sample was contained in an all-glass permeability cell and system, depicted in Figure 7; the hydrazine which permeated the samples was trapped out at liquid nitrogen temperature and then titrated with chloramine-T reagent.

A determination was made after a 96-hour period of test, a second collection vessel was attached immediately, and the test was continued for an additional 96 hours, since mass spectrometric studies have shown that the diffusion of propellants through thick samples may require more than three days before an equilibrium rate of diffusion is established.

The bladder samples were taken from a section near the girth weld and a section away from the girth weld. Additionally, a manufacturer's sample of SR722-70 provided by JPL was tested. As shown in Table 3, the reported values for the bladder samples are not consistent with the thicknesses involved; however, they are definitely within the more uniform rates obtained (in duplicate) for the "original" material. Thus, there is no apparent indication of increased permeability due to leaching out of fillers or reaction with minor components of the formulation.

MECHANICAL PROPERTY TESTS

Density Determinations

Density specimens were sectioned from the surface of the diaphragm which had been exposed to hydrazine and to nitrogen, and in both cases at areas near to and away from the girth weld. The results of the density determinations, performed by a simple water-displacement procedure, are given in Table 4. As shown, there is no perceptible difference in the density of specimens attributable to exposure to hydrazine or nitrogen. However, the EPR closest to the girth weld is definitely more dense than that away from the weld; this may be due either to EPR processing or tank assembly fabrication.

Hardness Determinations

Hardness was measured with a Shore Durometer; readings were taken on the A scale. Squares of material measuring at least 1.5 inches across were used in double thicknesses for the measurements; all readings were taken at least 1/2 inch away from any edge of the samples. As shown in Table 5, there is a distinct difference in hardness values between the sample taken near the girth weld and that taken away from the girth weld. The difference could be attributable either to the loss of plasticizer resulting from the heat of welding or to differences due to mode of manufacture.

Tensile and Elongation

Because of the continuously changing thickness of the diaphragm from the girth weld area to the area at the outlet barrier, it was necessary to cut micro specimens for the tensile tests in such a way as to assure as uniform a thickness as possible throughout the length of the specimens. The micro tensile specimens had an over-all length of 8 cm and a gage length of 3 cm; the gage width was 3 mm. They were tested at room temperature on an Instron Model TTCL tensile tester, using a crosshead speed of 1"/min. The values obtained for tensile strength and elongation at break are summarized in Table 6: no significant differences in specimens taken near the girth weld or away from the girth weld could be detected.

Table 1
RESULTS OF QUALITATIVE ANALYSES FOR
CATIONS IN EPR SR722-70 AFTER TEST

SAMPLE AREA	CATIONS DETECTED
Near girth weld	Zn, Ca, Fe, Ti
Away from girth weld	Zn, Ca, Fe

Table 2
EFFECT OF SUBSTANCES EXTRACTED FROM TEST
EPR SR722-70 ON THE DECOMPOSITION
OF HYDRAZINE AT 125°F
(48-hour Storage Test)

MEASUREMENT	N ₂ H ₄ CONTROL	N ₂ H ₄ WITH EPR EXTRACT
Ullage gas pressure at -196°C	0.5 near 1100	0.5 near 1100
Gas composition	Nitrogen; trace hydrogen	Nitrogen

Table 3
PERMEABILITY OF EPR SR722-70 AT 72°F
TO HYDRAZINE AT ONE ATMOSPHERE

SAMPLE LOCATION	SAMPLE THICKNESS	DURATION OF TEST	PERMEABILITY, mg/in ² -hr
Near girth weld	0.058"	96 hr	0.002
Near girth weld	same	2nd 96-hr interval	0.020
Away from girth weld	0.095"	96 hr	0.001
Away from girth weld	same	2nd 96-hr interval	0.002
Mfr's sample	0.051"	96 hr	0.033
Mfr's sample	same	2nd 96-hr interval	0.043

Table 4
 DENSITY DETERMINATIONS OF
 EPR SR722-70 AFTER TEST

SAMPLE AREA	REPLICATE-1	REPLICATE-2	AVERAGE
Away from girth weld, exposed to N ₂ H ₄	1.228	1.228	1.230
	1.230	1.229	
	1.230	1.233	
	1.231	1.231	
Away from girth weld, exposed to N ₂	1.232	1.234	1.231
	1.231	1.229	
	1.231	1.232	
	1.229	1.229	
Near girth weld, exposed to N ₂	1.235	1.239	1.240
	1.238	1.241	
	1.240	1.242	
	1.238	1.243	
Near girth weld, exposed to N ₂ H ₄	1.237	1.237	1.241
	1.238	1.242	
	1.242	1.245	
	1.241	1.244	

Table 5
 SHORE A HARDNESS DETERMINATIONS
 FOR EPR SR722-70

TEST NO.	AWAY FROM GIRTH WELD (0.063" thick)	NEAR GIRTH WELD (0.040" thick)
1	80	86
2	81	86
3	82	85
4	80	86
5	81	84
6	81	87
Av.	81	86

Table 6
 TENSILE AND ELONGATION VALUES
 FOR EPR SR722-70

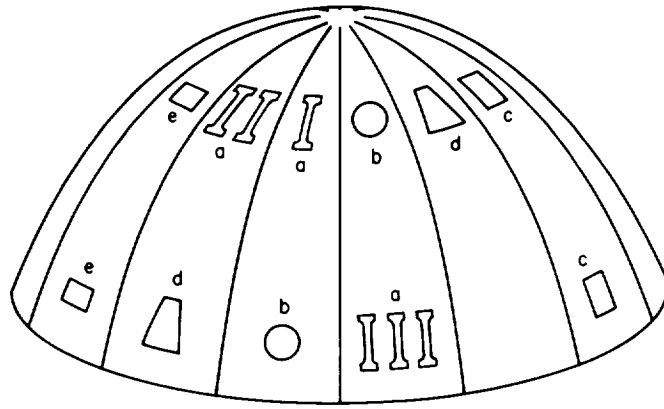
SAMPLE	SAMPLE AREA	THICKNESS	TENSILE STRENGTH, psi	% ELONGATION AT BREAK
1	Away from girth weld	0.059"	1450	280
2	Away from girth weld	0.058"	1400	250
3	Away from girth weld	0.058"	1330	240
Av.			1393	257
1	Near girth weld	0.047"	1550	280
2	Near girth weld	0.047"	1520	270
3	Near girth weld	0.047"	1450	260
Av.			1507	270



FIG. 4 PHOTOGRAPH OF THE EPR DIAPHRAGM (Hydrazine-Side) CUT AWAY FROM THE TITANIUM HEMISPHERE



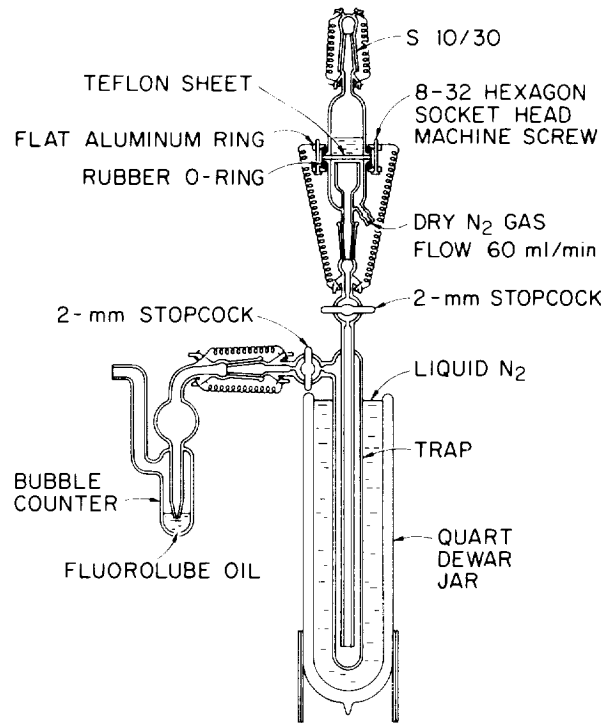
FIG. 5 PHOTOGRAPH OF THE INTERNAL AREA OF GENERANT TANK; NOTE DISCOLORATION RELATED TO DIAPHRAGM-RIB MARKS AND OTHER SPOTTY DEPOSITS



- a. TENSILE
- b. PERMEATION
- c. HARDNESS
- d. DENSITY
- e. CHEMICAL

TA-6063-124

FIG. 6 LOCATION OF SAMPLING AREAS FOR EPR DIAPHRAGM ANALYSES



TA-6063-128

FIG. 7 PERMEABILITY APPARATUS

III. TITANIUM TANK ANALYSIS

Samples for metallurgical analyses were taken from the girth weld area and locations away from the weld area. The locations of metallography samples as sectioned out of the titanium alloy hemisphere are shown in Figure 8 and the locations of the tensile test specimens are shown in Figure 9.

Sections were machined out of the 6Al-4V titanium alloy hemisphere, using accepted titanium-machining practice [4]. An 1/2-inch thick circular plate was prepared with a recessed annular groove to receive the open end of the hemisphere, and a clamp ring was made to secure the hemisphere to the plate. With this arrangement, the entire assembly could be aligned for machining. The hemisphere was held in a lathe and the valve section at the top of the hemisphere was removed. Then, a cone was inserted in the center hole and equidistant lines, 8° apart, were laid out from the base to the pole of the hemisphere to serve as references for the layout of the specimens.

A slitting saw on a milling machine was used to remove sample sections. The tools were operated at slow speeds and with sufficient soluble oil-water coolant to ensure that the specimens were not heated excessively. The separate pieces were then potted in Cerro Bend (m.p., 158°F) to prevent flexing of the specimens during final machining. All surfaces were finished with an end mill to an r.m.s. finish of 32 or better.

METALLOGRAPHY

The machine-cut metallographic specimens were polished under continuously-running water with progressively-finer grit sizes of silicon carbide, ranging from 180 to 600 grit. The macrospecimens, to be used unmounted, were then etched by immersion for 3-5 minutes in a conventional titanium macroetch (1 HF, 1.5 HCl, 2.5 HNO₃, 9.5 H₂O).

The specimens for photomicrography were mounted in "Cold Mount"--a room-temperature setting mounting medium--prior to the polishing operations described above. Subsequent treatment included:

- (1) Polishing with 3-micron diamond in a liquid carrier on a slow-speed wheel;
- (2) Polishing with Linde B on a microcloth under water on a slow-speed wheel;
- (3) Finished polishing on a Syntron vibratory-polisher with Linde B on a microcloth for 48 hours.

All photomicrography specimens were checked to ensure that metal flow had not occurred during the preparations. The surfaces were then etched with 10-second applications of a titanium alloy microetch (1 HF, 4 HNO₃, 96 H₂O).

Macrostructure

The generant tank outlet port (with the sieve-like barrier plate) which had been removed from the top of the hemisphere was cut longitudinally in half. After polishing and etching, the weld was studied under low magnification. The cross-section of the outlet port is shown in Figure 10, and a bottom view of the sieve-like barrier is shown in Figure 11. The weld zones showed no unusual macrostructure; a detailed discussion of the microstructure found in the welded areas is given later in this section.

The macro view of the girth weld in Figure 12 shows weld penetration into the back-up ring; the extent of weld penetration is similar to that noted in experimental studies [2]. Details of the microstructure are described in the following paragraphs.

Microstructure

For comparative purposes, samples were taken at the girth weld and at a distance away from the weld. Two samples were taken at each location so that microstructures could be viewed along two directions:

(1) transverse cross-section--perpendicular to the direction from the base to the top of the hemisphere, and (2) longitudinal--parallel to the base of the hemisphere.

Photomicrographs of the structure in the transverse section in the parent metal away from the weld area are shown in Figures 13 and 14, and those of the longitudinal section in Figures 15 and 16. Comparison of the photomicrographs in Figures 13 and 15 indicates that there is a tendency to preferred orientation of the grains along the longitudinal axis of the hemisphere. Observation of the parent metal indicates that it has a highly desirable microstructure with a well-dispersed alpha phase. The grain size averages between 15 to 20 microns.

Inspection of the 8X photomicrograph (Figure 17) of the longitudinal cross-section of the weld in the girth area revealed an interesting microstructure consisting of columnar grains extending down to the heat-affected zone (characterized by the smaller grain size) and a multiple banding appearing in the longitudinal direction about one-third of the distance down from the top surface of the weld. At a magnification of 20X (Figure 18), the nature of the bands is more evident, the amount of acicular structure being greater in the dark band areas. In Figure 19, the microstructure at 200X magnification shows the presence of a coarse-grained, transformed beta structure; a view at 1000X is given in Figure 20.

The girth weld is shown in the transverse direction at a magnification of 8X in Figure 21 and at 20X in Figure 22. The penetration of the weld extends about half-way into the back-up ring. The banding which was seen in the longitudinal cross-section (Figure 17) also appears here; it follows a circular path, with the center of the arc at about the top surface of the weld. Evidently, there were some variations or pulsations in the welding process that caused changes in the temperature gradient and corresponding variations in the microstructure. The edge of the heat-affected zone is shown in Figure 23, and the weld area itself with the transformed beta structure may be seen in Figure 24; a view of the latter at higher magnification is given in Figure 25.

MECHANICAL PROPERTY DETERMINATIONS

Mechanical-property specimens were taken from the locations on the hemisphere shown in Figure 9: (1) transverse to the girth weld, with the weld passing approximately across the center of the gage section of the specimen (specimens 1 and 2); (2) longitudinally along the girth weld so that the entire gage section consisted of girth-weld material (specimens 3 and 4); and (3) transverse to the girth weld in an area away from the weld (specimens 10 and 11).

After the specimen blanks were cut out of the hemisphere, they were machined to the dimensions shown in Figure 26. Because of the spherical curvature of the hemisphere and the thin wall-thickness, it was not possible to machine tensile specimens of standard dimensions. This factor would make the results obtained in this analysis not strictly comparable to those obtained by the use of standard specimens. Every effort was made to design the specimens to minimize the effect of differences in geometry on mechanical properties. Since ASTM standards do not provide for sub-size flat tension specimens, reference was made to British Standards [5] and to a discussion on specimen geometry effects on elongation [6, 7].

After the tensile specimens were machined to a finish of 32, they were polished along the longitudinal axis on 180-grit silicon carbide paper, with ample flowing water, to eliminate any scratches that might serve as stress inducers. They were tested on an Instron Model TTCL tensile testing machine. A one-inch clamp-on strain gage was used to measure the strain, and a stress-strain curve was recorded directly. In addition, tests were performed with load-time recording and the strain was determined from the movement of the cross-head. The elongation was determined with reference to one-inch gage marks made on the gage length of the specimen; measurements were made before and after each run and checked against the elongation recorded on the chart. After the yield strength of the specimen was recorded, the strain gage was removed and the test was continued to failure of the specimen.

The test results are summarized in Table 7. It should be noted that the yield values of parent metal run slightly lower than the minimum values given in JPL Spec. No. 30209B [1], which are indicated as notes to Table 7. Since there is no knowledge of tensile data for the actual titanium alloy used in fabrication or of the exact nature of fabrication processes for this particular vessel, and the specifications are based on different test-specimen geometry than that used in this analysis, no positive statement can be made to indicate any deterioration of tensile properties caused by environmental conditions. However, the data in Table 7 suggest that the metal has suffered no gross alteration of properties.

Hardness

Microhardness measurements were made for the welded and parent materials with a Vickers hardness tester, using a 200-g load. The data are summarized in Table 8; the average of ten readings for samples from each area furnishes values of 316 DPH for the parent metal and 338 DPH for the weld metal. This meets the specifications for the weld hardness to be not more than 30 Diamond Pyramid Hardness numbers than the parent metal.

Table 7

MECHANICAL PROPERTIES OF SELECTED AREAS OF T1-6A1-4V GENERANT TANK

SPECIMEN ¹ NO.	DESCRIPTION	YIELD STRENGTH (0.2% Offset), psi	ULTIMATE TENSILE ² STRENGTH, psi	% ELONGATION ² (1-inch gage length)	% REDUCTION ² IN AREA
1	Transverse section across girth weld	120,200	142,500	12.0	32.5
2	Same	120,400	138,300	10.3	32.9
3	Longitudinal section within girth weld	120,800	149,600	10.3	21.6
4	Same	122,500	152,000	8.2	18.1
10	Transverse section away from weld	123,500	140,200	7.9	35.4
11	Same	123,300	141,500	8.2	31.0

NOTES

1. Location of specimen on hemisphere shown in Fig. 9.
2. Specifications for Mechanical Properties, JPL Spec. No. 30209B[1].

CONDITION	YIELD STRENGTH (0.2% Offset), psi	ULTIMATE STRENGTH, psi	ELONGATION	REDUCTION IN AREA
Annealed	125,000 min 140,000 max	135,000 min 150,000 max	12% min	30% min
Heat-treated	150,000 min 165,000 max	160,000 min 175,000 max	10% min	30% min

Table 8

MICROHARDNESS MEASUREMENTS OF PARENT METAL AND
WELDED METAL IN 6A1-4V TITANIUM HEMISPHERE
(200-g load; Vickers Diamond Pyramid Hardness)

PARENT METAL	WELDED METAL
306	330
329	341
310	341
312	355
313	334
353	336
321	339
294	329
308	341
286	336
Av. 316	Av. 338

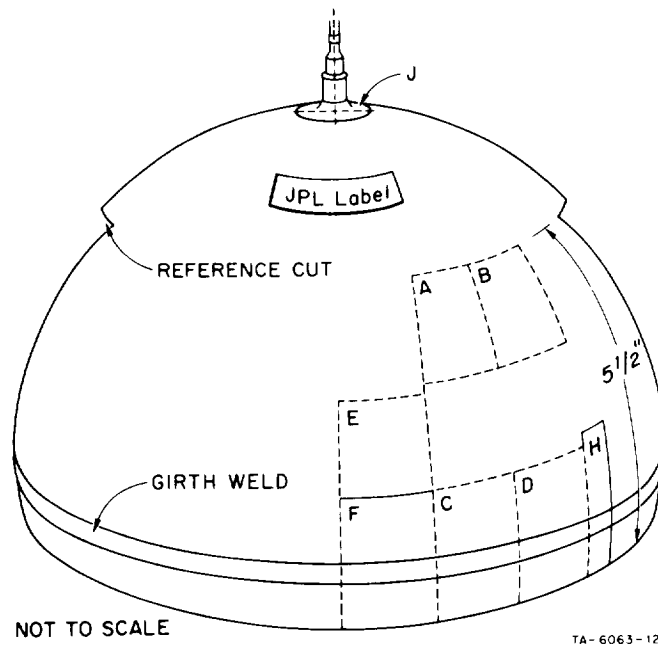


FIG. 8 LOCATION OF METALLOGRAPHY SPECIMENS

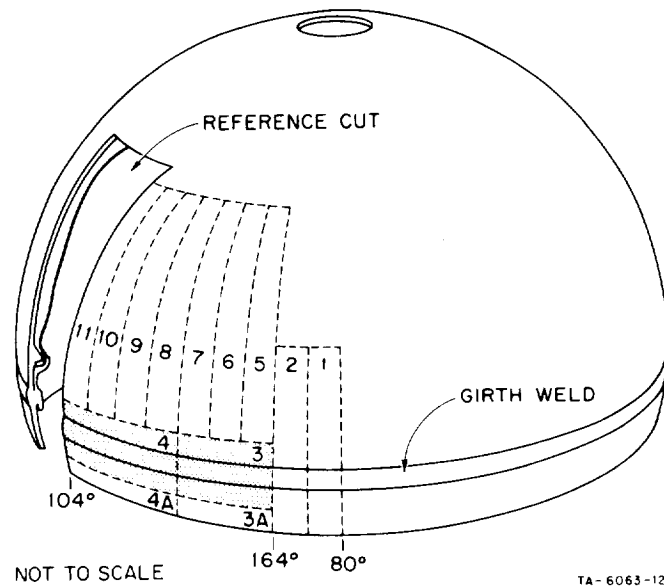


FIG. 9 LOCATION OF TITANIUM TENSILE SPECIMENS

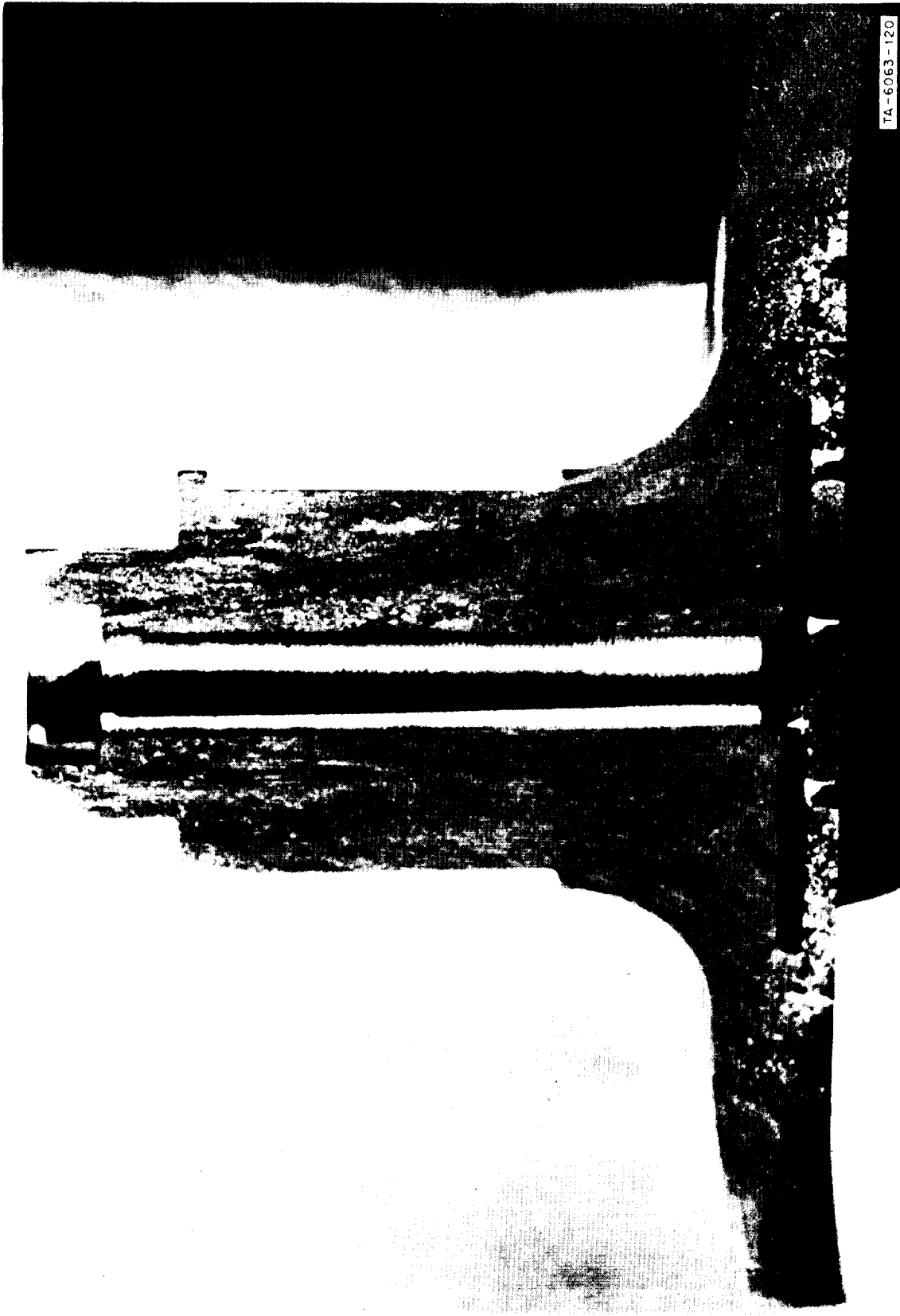


FIG. 10 CROSS-SECTION OF GENERANT TANK OUTLET PORT AND BARRIER PLATE;
MAGNIFICATION, 5X. (Macroetch, 1 HF, 1.5 HCl, 2.5 HNO₃, 95 H₂O)

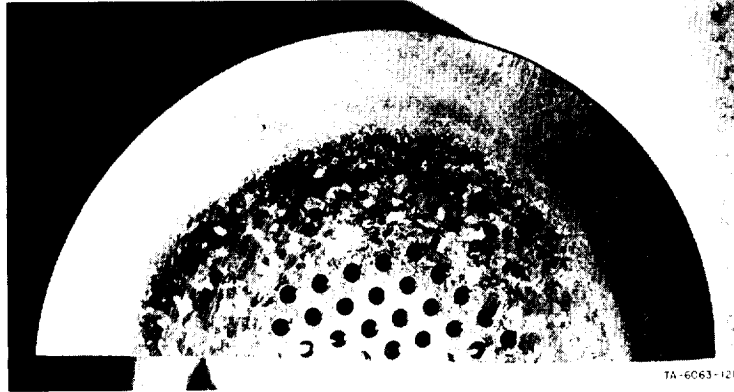


FIG. 11 BOTTOM VIEW OF SIEVE-LIKE BARRIER LEADING TO GENERANT TANK OUTLET PORT; MAGNIFICATION, 2X. (Macroetch, 1 HF, 1.5 HCl, 2.5 HNO₃, 95 H₂O)

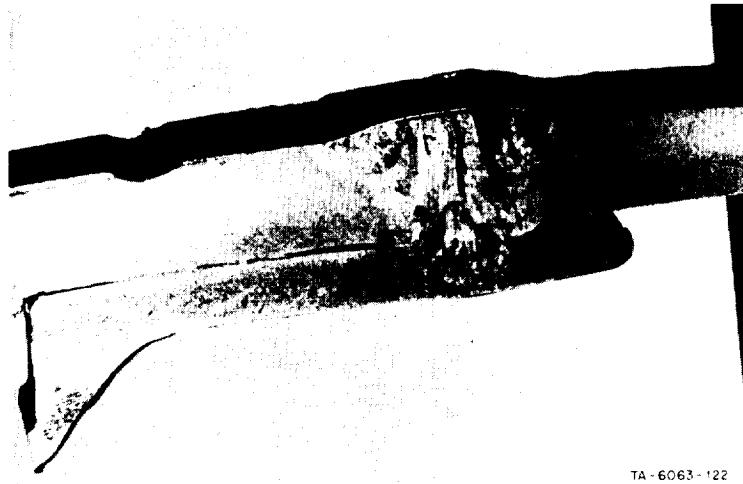


FIG. 12 CROSS-SECTION THROUGH GIRTH WELD AREA; MAGNIFICATION, 2.5X (Macroetch, 1 HF, 1.5 HCl, 2.5 HNO₃, 95 H₂O)

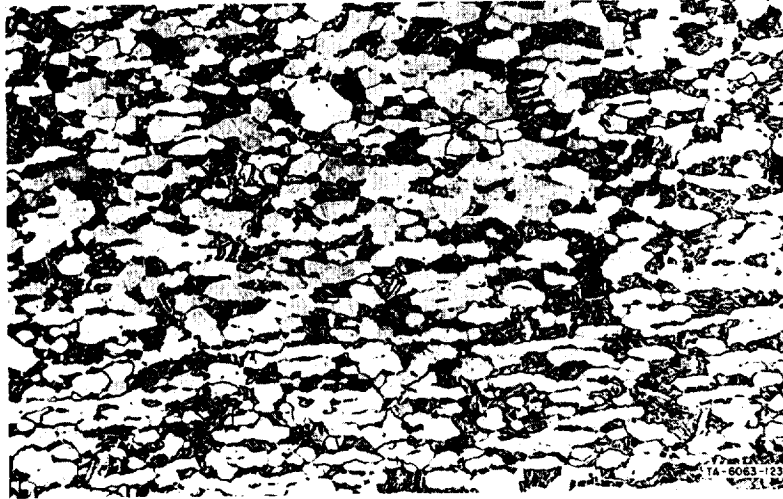


FIG. 13 PHOTOMICROGRAPH OF TRANSVERSE CROSS-SECTION OF HEMISPHERE AWAY FROM THE WELD AREA; MAGNIFICATION, 250X. (Etchant, 1 HF, 4 HNO₃, 95 H₂O, swab 10 seconds)



FIG. 14 PHOTOMICROGRAPH OF TRANSVERSE CROSS-SECTION OF HEMISPHERE AWAY FROM THE WELD AREA; MAGNIFICATION, 1000X

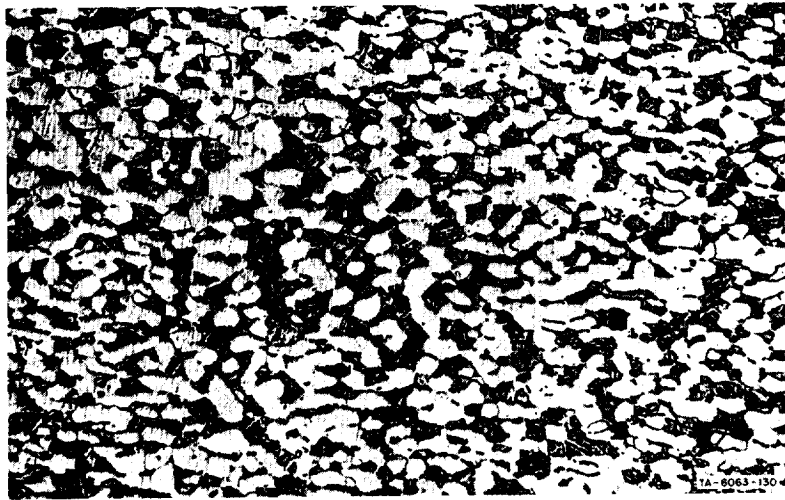


FIG. 15 PHOTOMICROGRAPH OF LONGITUDINAL CROSS-SECTION AWAY FROM THE WELD AREA; MAGNIFICATION, 250X (Etchant : 1 HF, 4 HNO₃, 95 H₂O swab 10 seconds)



FIG. 16 PHOTOMICROGRAPH OF LONGITUDINAL CROSS-SECTION AWAY FROM THE WELD AREA; MAGNIFICATION, 1000X



FIG. 17 MACROPHOTO OF LONGITUDINAL SECTION THROUGH GIRTH WELD;
MAGNIFICATION, 8X. (Etchant: 1 HF, 4 HNO₃, 95 H₂O, swab 10 seconds)



FIG. 18 PHOTOMICROGRAPH AT CENTER LINE OF LONGITUDINAL
SECTION THROUGH GIRTH WELD; MAGNIFICATION, 20X
(Etchant: 1 HF, 4 HNO₃, 95 H₂O, swab 10 seconds)

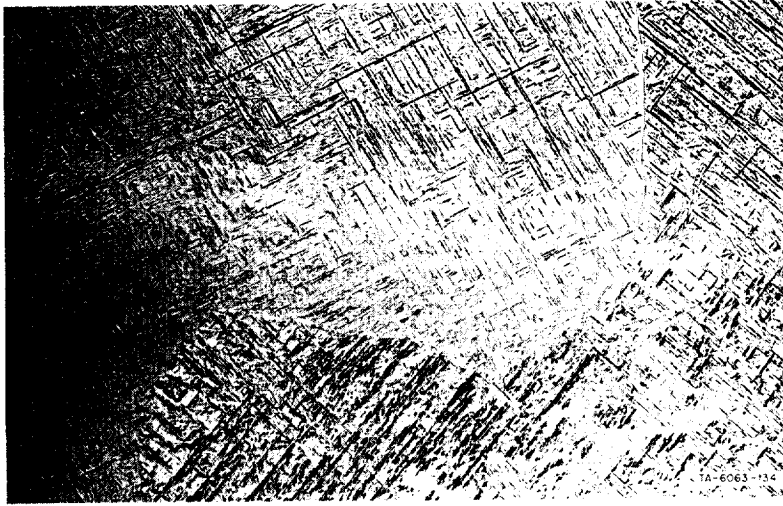


FIG. 19 PHOTOMICROGRAPH OF LONGITUDINAL SECTION THROUGH GIRTH WELD; MAGNIFICATION, 200X

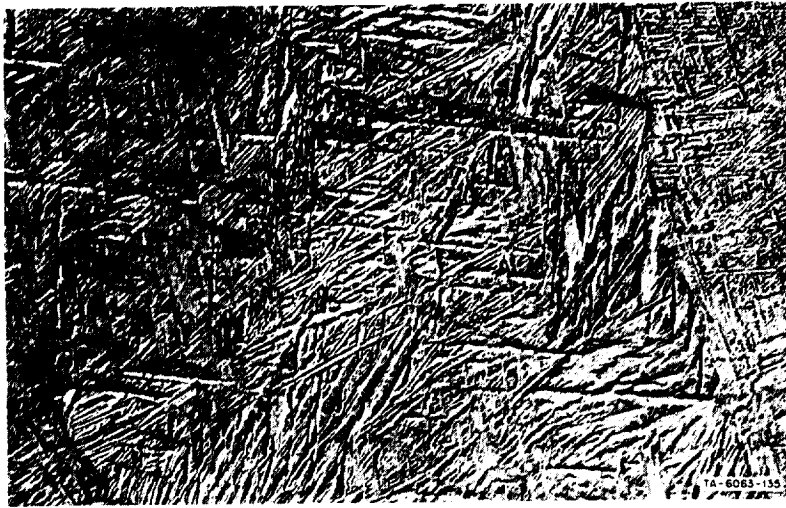


FIG. 20 PHOTOMICROGRAPH OF LONGITUDINAL SECTION THROUGH GIRTH WELD; MAGNIFICATION, 1000X

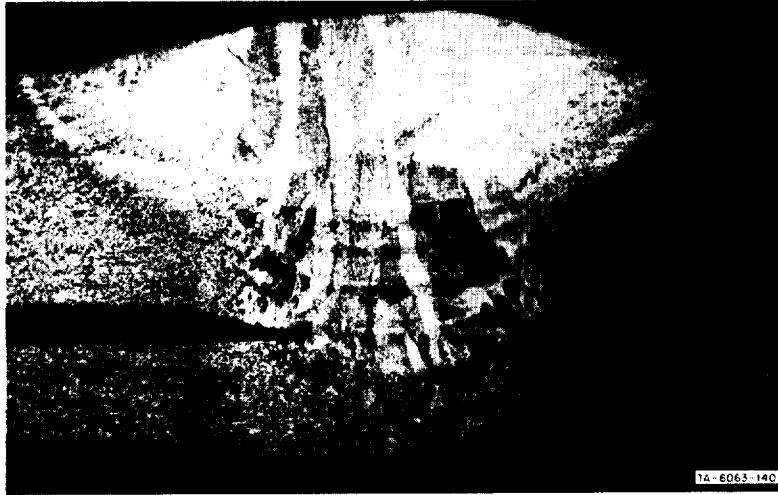


FIG. 21 MACROPHOTO OF TRANSVERSE CROSS-SECTION OF GIRTH WELD; WALL OF HEMISPHERE TO THE LEFT AND BACK-UP RING ON THE RIGHT; MAGNIFICATION, 8X. (Etchant: 1 HF, 4 HNO₃, 95 H₂O, swab 10 seconds)

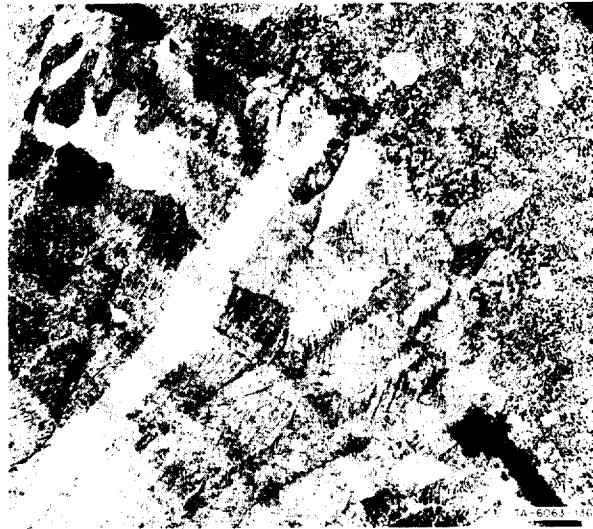


FIG. 22 PHOTOMICROGRAPH OF GIRTH WELD AT JOINT AREA BETWEEN WALL OF HEMISPHERE AND BACK-UP RING; MAGNIFICATION, 20X. (Etchant: 1 HF, 4 HNO₃, 95 H₂O)

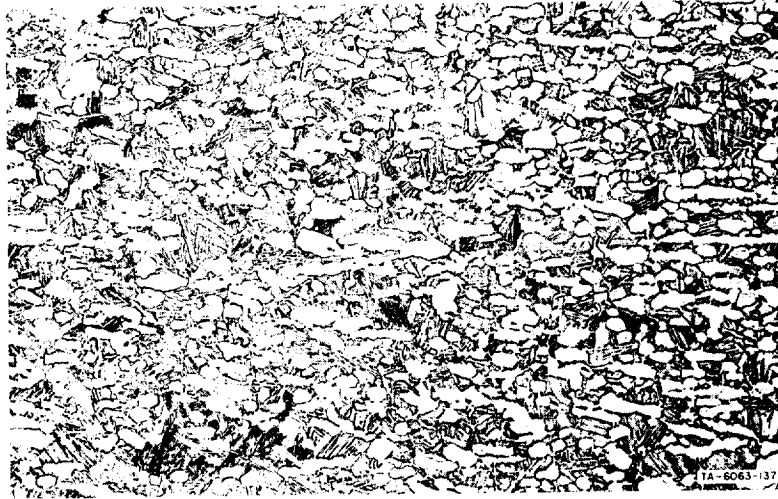


FIG. 23 PHOTOMICROGRAPH OF EDGE OF HEAT-AFFECTED ZONE OF WELD SHOWN IN FIGURE 22; MAGNIFICATION, 200X. (Etchant: 1 HF, 4 HNO₃, 95 H₂O)



FIG. 24 PHOTOMICROGRAPH OF GIRTH WELD; MAGNIFICATION, 200X (Etchant: 1 HF, 4 HNO₃, 95 H₂O, swab 10 seconds)

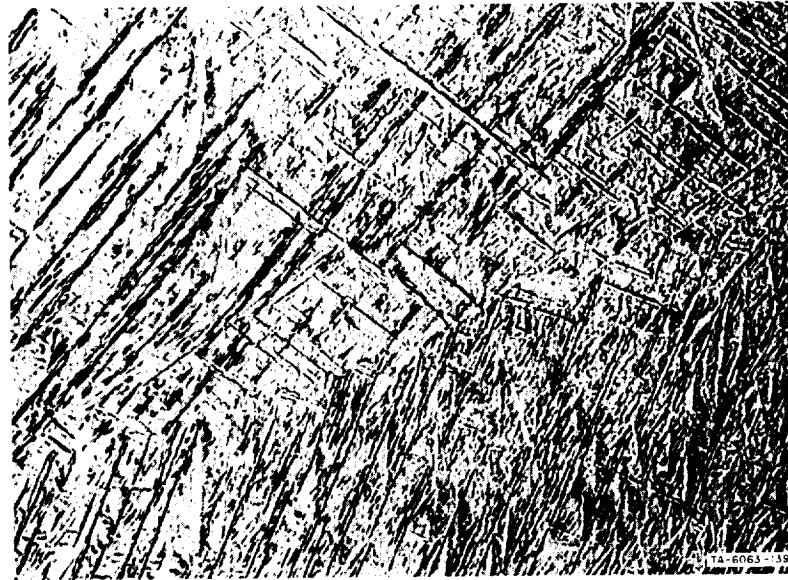
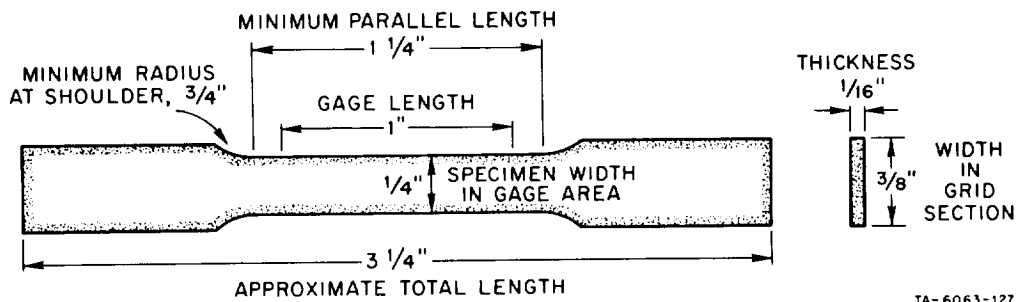


FIG. 25 PHOTOMICROGRAPH OF GIRTH WELD; MAGNIFICATION, 1000X



TA-6063-127

FIG. 26 DIMENSIONS OF TITANIUM TENSILE TEST SPECIMENS

IV. SUMMARY AND CONCLUSIONS

Preliminary examination of the partial SN/004 generant tank received at SRI revealed no obvious defects in the parent metal, in the girth or outlet welds, in the bond of the diaphragm at the girth weld, nor in the diaphragm itself.

The surfaces of the titanium hemisphere and the EPR diaphragm which had been in contact with hydrazine showed apparent effects of passive reaction, that is, leaching of substances from the EPR diaphragm material.

EPR Diaphragm

It has been demonstrated that materials leached-out of the SR722-70 elastomer by hydrazine have no apparent effect toward accelerating the decomposition of hydrazine in an accelerated 24-hour test. The small differences in the mechanical properties of the diaphragm material at different areas are attributable rationally to modes of manufacture and/or differences in thicknesses of sample sections. However, it may be noted that some of the mechanical properties are at variance with measurements made on analagous materials submitted by the manufacturer for test in other programs:

<u>Test Sample</u>	<u>Tensile Strength, psi</u>	<u>Elongation, %</u>	<u>Hardness, Shore A</u>	<u>Ref.</u>
EPR diaphragm	1393-1507	257-270	81-86	--
Mfr. sample	--	--	65	[2]
Mfr. sample	2488	269	77	[8]
Mfr. sample	2202	326	77	--

The cited data would imply either a nonuniformity of processing or more likely an actual embrittlement of the diaphragm material because of exposure to hydrazine or test conditions.

The end-user must determine whether the post-test mechanical and physical properties are acceptable for contemplated space storage. However, it is noted that the tensile strength of the material at 1393-1507 psi is distinctly inferior to that of the original material. Also, since an unmanned spacecraft for planetary exploration may also be subjected to a heat-sterilization procedure, the following information is offered on the mechanical properties of SR722-70 after high-temperature cycles in air and in vacuum [8]:

<u>Property</u>	<u>Control</u>	<u>Postcured 24 Hr in air at 150°C</u>	<u>Stored at 10⁻⁶ Torr 300 Hr at 135°C</u>
Tensile Strength, psi	2488	1571	2294
Elongation, %	269	195	245
Hardness, Shore A	77.0	77.5	80.5

The assembled data for the diaphragm material indicate that the mode of fabrication and assembly within the generant tank is acceptable. On the other hand, recommendation of the SR722-70 for long-term storage with hydrazine is doubtful in view of the apparent embrittlement, loss in tensile strength, and the possible effects of leached substances on hydrazine decomposition over a long period of time. More extensive and controlled testing is required before a positive recommendation can be made.

Titanium Alloy Tank

Metallographic studies indicated no nonconformities of surface features of the metal, such as might result from slow dissolution of metal or reaction with deposited foreign matter. Detailed inspection of the welded and parent metal areas reveals only the type of microstructure that one could expect under the conditions of fabrication.

A critical review of the metallographic data and the results of mechanical property tests indicate that the materials and fabrication of the prototype generant tank are acceptable for continued use in the environment under consideration, and suggest that any deterioration which may have taken place during test is trivial and is not localized.

V. REFERENCES

1. Jet Propulsion Laboratory, "Process Specifications No. 30209; Spacecraft Flight Equipment: Titanium Alloy, 6Al-4V Pressure Vessel," Change B, 24 May 1961.
2. O. F. Keller and L. R. Toth, Jet Propulsion Laboratory, "ALPS Generant Tank and Cell Assembly," Tech. Report No. 32-865, February 28, 1966.
3. R. N. Porter and H. B. Stanford, Jet Propulsion Laboratory, "Propellant Expulsion in Unmanned Spacecraft," Tech. Report No. 32-899, July 1, 1966.
4. C. T. Olofson, "The Machining of Titanium," in Titanium-1966, Lectures Given at a Norair Symposium, March 28-29, 1966, DMIC-Memorandum 215, September 1, 1966.
5. British Standard 18:1962, "Methods for Tensile Testing of Metals," including Amendments No. 1 and No. 2, 1966, British Standards Institution.
6. C. B. Kula and N. H. Fahey, "Effect of Specimen Geometry on Determination of Elongation in Sheet Tension Specimens," Materials Research and Standards, 1 (8), 631 (1961).
7. E. E. Weismantel, "Discussion of Paper [Reference (3) above]," Materials Research and Standards, 2 (1), 20 (1962).
8. R. F. Muraca and J. S. Whittick, Stanford Research Institute, "Polymers for Spacecraft Applications," Final Report, JPL Contract 950745, September 15, 1967.

STANFORD RESEARCH INSTITUTE



Main Offices and Laboratories

333 Ravenswood Avenue
Menlo Park, California 94025
(415) 326-6200
Cable: STANRES, Menlo Park
TWX: 910-373-1246

Regional Offices and Laboratories

Southern California Laboratories

820 Mission Street
South Pasadena, California 91030
(213) 799-9501 • 682-3901
TWX: 910-588-3280

SRI-Washington

1611 North Kent Street, Rosslyn Plaza
Arlington, Virginia 22209
(703) 524-2053
Cable: STANRES, Washington, D.C.
TWX: 710-955-1137

SRI-New York

200 E. 42nd Street
New York, New York 10017
(212) 661-5313

SRI-Huntsville

Missile Defense Analysis Office
4810 Bradford Blvd., N.W.
Huntsville, Alabama 35805
(205) 837-3050
TWX: 810-726-2112

SRI-Chicago

10 South Riverside Plaza
Chicago, Illinois 60606
(312) 236-6750

SRI-Europe

Pelikanstrasse 37
8001, Zurich, Switzerland
27 73 27 or 27 81 21
Cable: STANRES, Zurich

SRI-Scandinavia

Skeppargatan 26
Stockholm O, Sweden
600-226; 600-396 600-475

SRI-Japan

Edobashi Building, 8th Floor
1-6, Nihonbashi Edobashi
Chuo-ku, Tokyo
Tokyo 271-7108
Cable: STANRESARCHI, Tokyo

SRI-Southeast Asia

Bangkok Bank Building
182 Sukhumvit Road
Bangkok, Thailand
Bangkok 910-181
Cable: STANRES, Bangkok

Representatives

Canada

Cyril A. Ing
Olympia Square
797 Don Mills Road
Toronto, Ontario, Canada
(416) 429-2162

France

Roger Godino
94, Boulevard du Montparnasse
75 Paris 14^e, France
633 37 30

Portugal

J. Gasparinho Correia
Avenida João XXI, 22-3 Esq.
Lisbon, Portugal
72 64 87

Italy

Lorenzo L. Franceschini
Via Macedonio Melloni 49
20129, Milan, Italy
72 32 46

